

# Harmful algae bloom monitoring via a sustainable, sail-powered mobile platform for in-land and coastal monitoring

Jordon S. Beckler<sup>1\*</sup>, Ethan Arutunian<sup>2</sup>, Robert D. Currier<sup>3</sup>, Eric Milbrandt<sup>4</sup>, Scott Duncan<sup>2</sup>

<sup>1</sup>Harbor Branch Oceanographic Institute, Florida Atlantic University, United States, <sup>2</sup>Navocean, United States, <sup>3</sup>Gulf of Mexico Coastal Ocean Observing System Regional Association, United States, <sup>4</sup>Sanibel Captiva Conservation Foundation, United States

*Submitted to Journal:*  
Frontiers in Marine Science

*Specialty Section:*  
Ocean Observation

*Article type:*  
Technology Report Article

*Manuscript ID:*  
437032

*Received on:*  
15 Nov 2018

*Frontiers website link:*  
[www.frontiersin.org](http://www.frontiersin.org)

In review

### *Conflict of interest statement*

The authors declare that the research was conducted in the absence of any commercial or financial relationships that could be construed as a potential conflict of interest

### *Author contribution statement*

JB authored the manuscript, provided scientific oversight, and participated in field campaigns, EA is the lead designer of the autonomous vehicle hardware and software, RC developed live data visualization interface, EM coordinated field campaigns, and SD designed the sailboat and conducted deployments.

### *Keywords*

Autonomous & remotely-operated vehicle, harmful algal bloom, Mapping, *Karenia brevis* HABs, CDOM, Ocean observation, West Florida Shelf, surface vehicle

### *Abstract*

Word count: 222

Harmful algae blooms (HAB) in coastal marine environments are increasing in number and duration, pressuring local resource managers to implement mitigation solutions to protect human and ecosystem health. However, insufficient spatial and temporal observations create uninformed management decisions. In order to better detect and map blooms, as well as the environmental conditions responsible for their formation, long-term, unattended observation platforms are desired. In this article, we describe a new cost-efficient, autonomous, mobile platform capable of accepting several sensors that can be used to monitor harmful algae blooms in near real-time. The Navocean autonomous sail-powered surface vehicle is deployable by a single person from shore, capable of waypoint navigation in shallow and deep waters, and powered completely by renewable energy. We present results from three surveys of the Florida Red Tide harmful algae bloom (*Karenia brevis*) of 2017-2018. The vessel made significant progress towards waypoints regardless of wind conditions while underway chl. a measurements revealed HAB bloom patches and CDOM and turbidity provided environmental contextual information. While the autonomous sailboat directly adds to our HAB monitoring capabilities, the boat can also help to ground-truth and thus improve satellite monitoring of HABs. Finally, several other pending and future use cases for coastal and inland monitoring are discussed. To our knowledge, this is the first demonstration of a sail-driven vessel used for coastal HAB monitoring.

### *Funding statement*

This work was supported in part by a National Academies Gulf Research Program Early Career Fellowship award #2000007281 that supporting salary and supplies, and the Gulf of Mexico Coastal Ocean Observation System #NA16NOS0120018 that supported salaries.

### *Ethics statements*

(Authors are required to state the ethical considerations of their study in the manuscript, including for cases where the study was exempt from ethical approval procedures)

*Does the study presented in the manuscript involve human or animal subjects:* No

### *Data availability statement*

Generated Statement: All datasets generated for this study are included in the manuscript and the supplementary files.

# Harmful algae bloom monitoring via a sustainable, sail-powered mobile platform for in-land and coastal monitoring

1 **Jordon S. Beckler<sup>1\*,‡</sup>, Ethan Arutunian<sup>2</sup>, Bob Currier<sup>3</sup>, Eric Milbrandt<sup>4</sup>, Scott Duncan<sup>2</sup>**

2 <sup>1</sup>Geochemical Sensing Laboratory, FAU Harbor Branch Oceanographic Institute, Ft. Pierce, Florida,  
3 USA

4 <sup>2</sup>Navocean Inc., Seattle, Washington, USA

5 <sup>3</sup>Gulf of Mexico Coastal Ocean Observation System (GCOOS), Texas A&M University, College  
6 Station, Texas, USA

7 <sup>4</sup>SCCF Marine Laboratory, Sanibel Captiva Conservation Foundation, Sanibel, Florida, USA

8

9 **\* Correspondence:**

10 Corresponding Author

11 [jbeckler@fau.edu](mailto:jbeckler@fau.edu)

12 **‡Formerly:**

13 Ocean Technology Research Program, Mote Marine Laboratory, Sarasota, Florida, USA

14 **Keywords: Autonomous & Remotely Operated Vehicle<sup>1</sup>, Harmful Algal Bloom<sup>2</sup>, Mapping<sup>3</sup>,**  
15 ***Karenia brevis* HABs<sup>4</sup>, CDOM<sup>5</sup>, Turbidity<sup>6</sup>, West Florida Shelf<sup>7</sup>, Surface Vehicle<sup>8</sup>**

16 **Abstract**

17 Harmful algae blooms (HAB) in coastal marine environments are increasing in number and duration,  
18 pressuring local resource managers to implement mitigation solutions to protect human and  
19 ecosystem health. However, insufficient spatial and temporal observations create uninformed  
20 management decisions. In order to better detect and map blooms, as well as the environmental  
21 conditions responsible for their formation, long-term, unattended observation platforms are desired.  
22 In this article, we describe a new cost-efficient, autonomous, mobile platform capable of accepting  
23 several sensors that can be used to monitor harmful algae blooms in near real-time. The Navocean  
24 autonomous sail-powered surface vehicle is deployable by a single person from shore, capable of  
25 waypoint navigation in shallow and deep waters, and powered completely by renewable energy. We  
26 present results from three surveys of the Florida Red Tide harmful algae bloom (*Karenia brevis*) of  
27 2017-2018. The vessel made significant progress towards waypoints regardless of wind conditions  
28 while underway chl. *a* measurements revealed HAB bloom patches and CDOM and turbidity  
29 provided environmental contextual information. While the autonomous sailboat directly adds to our  
30 HAB monitoring capabilities, the boat can also help to ground-truth and thus improve satellite  
31 monitoring of HABs. Finally, several other pending and future use cases for coastal and inland  
32 monitoring are discussed. To our knowledge, this is the first demonstration of a sail-driven vessel  
33 used for coastal HAB monitoring.

## 34 1 Introduction

35 In the last few decades, harmful algae blooms (HABs) have increased in number, intensity, and  
36 duration due to cultural eutrophication, increasing rainfall, and warming temperatures (Brand and  
37 Compton, 2007; O’Neil et al., 2012). Through the generation of toxins or by creating locally hypoxic  
38 conditions, HAB effects can range from acute sickness and respiratory irritation potentially affecting  
39 local economies (Backer et al., 2010; Hoagland et al., 2009; Kirkpatrick et al., 2006), to massive  
40 marine fish and mammal mortality events (Gannon et al., 2009; Scholin et al., 2000), or even to  
41 chronic human poisoning and death through ingestion of contaminated shellfish or drinking water  
42 (Carmichael, 2001; Fleming et al., 2002; Reich et al., 2015). HAB blooms are most frequently  
43 observed and anthropogenically detrimental in coastal or in-land marine and freshwater bodies  
44 (Anderson et al., 2002), for example in areas with coastal recreation, fishing, mari/aquaculture, and  
45 drinking water intake systems. Recent years have experienced superlative HAB events with  
46 unparalleled public recognition, for example the summer of 2014 and 2016 *Microcystis aeruginosa*  
47 blue-green cyanoblooms in Lake Erie and the Indian River Lagoon (Florida) (Smith et al., 2015;  
48 Stockley et al., 2018) that poisoned drinking water and decreased property values, respectively, the  
49 *Pseudo-nitzschia* bloom of 2015 in California waters that led to the closing of the dungeoness crab  
50 fishing season (McCabe et al., 2016), and the 2017-2018 *Karenia brevis* bloom in west Florida  
51 (ongoing as of the time of writing) that has led to a declaration of a state of emergency. This “Florida  
52 Red Tide” bloom is poised to be the worst on record and has brought an unprecedented amount of  
53 national attention to this particular HAB (Ducharme, 2018).

54 To plan for and mitigate the occurrence and effects of HABs, it is ideal to both monitor the algae  
55 and/or toxins directly and collect additional ancillary information regarding the chemical and  
56 physical ecology of the ecosystems. Traditional routine monitoring is inherently expensive, time  
57 consuming, and the spatial and temporal resolution of discrete measurements in many HAB-prone  
58 regions is often not sufficient to elucidate bloom causes or properly initiate models. According to a  
59 recent HAB scientist community consensus, an observing system consisting of satellite, moored, and  
60 mobile data collection platforms will most likely emerge as the most effective holistic approach  
61 (Bowers and Smith, 2017). Careful consideration must be given to important tradeoffs existing  
62 between sensor specificity targets (e.g. pigments, species, or toxins) and platform compatibility (i.e.  
63 fixed location versus mobile), which together determine cost, sampling resolution, and reliability. For  
64 example, while satellite-based remote sensing is inexpensive, the technique suffers from insufficient  
65 temporal (e.g. daily) and spatial resolution (e.g. ~ 1km), non-species specificity, and interferences  
66 from the seafloor, suspended sediment, and clouds. Fixed-location, unattended monitoring devices  
67 (i.e. shoreline or moorings) have drastically advanced the temporal resolution of data collection,  
68 especially at the species level (Smith et al., 2015; Stockley et al., 2018), but the installation of enough  
69 locations to provide sufficient spatial resolution is cost-prohibitive (Shapiro et al., 2015). Given the  
70 vertical heterogeneity of HABs, 3-dimensional monitoring platforms, such ocean-going autonomous  
71 underwater vehicle buoyancy gliders, are promising and have been successfully deployed in near-  
72 shore and open ocean environments (Robbins et al., 2006). However, the submerged nature of these  
73 vehicles creates communications, power, and reliability constraints that currently limit sensor options  
74 and few species-level options exist. In turn, 2-dimensional Autonomous Surface Vehicles (ASV)  
75 such as those powered by sail or waves e.g. “Wave Gliders” or Sairdrone (Daniel et al., 2011; Mordy  
76 et al., 2017) may alleviate these constraints and are arguably more favorable for more complex  
77 instrumentation. However, to our knowledge, all existing long-duration autonomous vehicles are not  
78 designed to operate effectively in shallow and/or near-shore waters less than a few meters depth, their  
79 size, form or performance prohibit shallow water operation, and their operation is challenging for  
80 non-expert resource managers.

81 For over a decade on the southwest Florida Shelf, fixed location, species-specific optical devices (i.e.  
82 Optical Phytoplankton Discriminators; OPD) have been employed as part of a State of Florida and  
83 NOAA funded HAB observatory (Sarasota Operations of the Coastal Ocean Observing Lab of Mote  
84 Marine Laboratory; SO-COOL). Additionally, AUVs (Slocum gliders) outfitted with either an OPD  
85 or a chl. *a* fluorometer are also routinely used to locate and track *K. brevis* HABs (Shapiro et al.,  
86 2015). While these efforts have yielded valuable insights into the conditions surrounding HAB bloom  
87 formation, these glider operations have presented challenges over the years. Deployments are  
88 logistically challenging, requiring an initial transit to deeper waters, and once deployed, a minimum  
89 depth limitation of 10 meters (i.e. 20 km from the coast). Finally, cost has prohibited sufficient  
90 spatial and temporal coverage, and deployments have been met with unanticipated buoyancy-related  
91 operational challenges such as aborts due to nuisance “suckerfish” attaching and sinking gliders (i.e.  
92 remora fish).

93 In 2016, Mote Marine Laboratory began a collaboration with Navocean, Inc., to utilize their  
94 autonomous sail-powered surface vehicle for *K. brevis* bloom monitoring. Navocean offers small, 2-  
95 m in length vessels that are reliable, and can accept versatile sensors. Navocean boats fill a current  
96 niche in both the Autonomous Surface Vehicle (ASV) and the HAB mapping markets, being  
97 powered solely from renewable sources, inexpensive, navigable in shallow waters (> 1 m), and  
98 deployable from shore by a single person. To demonstrate proof of concept for HAB monitoring, a  
99 Navocean *Nav2* boat was outfitted with a 3-channel fluorometer (Turner Designs) configured to  
100 measure chl. *a* as a proxy for phytoplankton pigments, as well as CDOM and turbidity to provide  
101 ancillary environmental information. The boat was deployed for periods of up to one week in the  
102 Winter of 2017, during the start of what has become one of the worst *K. brevis* blooms on record.  
103 This work describes the system design, testing, and in situ validation, then discusses other potential  
104 applications for HAB monitoring and other environmental applications for this unique vehicle.

## 105 2 Vessel Design and Operation

106 The *Nav2* ASV (**Figure 1**) is small, lightweight, easy to launch/land and non-hazardous in the event  
107 of collision. The base cost is < \$75k and daily operating costs are primarily satellite data fees (\$25 to  
108 \$55 typical). The vessel is 2 m in length, drafts 0.75 m, and weighs between 38 and 45 kg.  
109 (depending on battery configuration). The boat has a fiberglass shell with a thick foam core  
110 providing reserve buoyancy. The fin keel and rudder are designed to shed seaweed and debris and  
111 have proven resistant to tangling in fishing lines and lobster and crab gear in previous missions. The  
112 2 m tall mast has a bright orange sail for high visibility. A “Bermudan” style rig consists of a  
113 reinforced carbon mast with high strength Dacron sails (main sail and a small jib) and chafe-resistant  
114 lines. The *Nav2* is outfitted with an Airmar 200WX IPX7 marine grade meteorological sensor for  
115 wind speed and direction for navigation/scientific purposes, as well as air temperature and barometric  
116 pressure for scientific purposes. The *Nav2* is controlled via an iOS application (iPad or iPhone) that  
117 is in constant communication to the boat using Wi-Fi, Cellular, or Iridium satellite in either manual  
118 mode for line of sight control or autonomous mode for waypoint navigation (**Figure 2**), which  
119 includes up-wind tacking in variable wind and sea states. A small electric thruster also provides back-  
120 up propulsion for flat calm-wind conditions and for facilitating deployment and recovery, as needed.  
121 The standard battery bank consists of up to 5 x LiFePO<sub>4</sub> batteries, for a total of 100 A hr and 1200 W  
122 hr. Nominal 35 Watt solar panels provide solar recharge of the onboard battery bank for long  
123 duration missions (up to several months).

124 A 3-channel fluorometer (Turner Designs Cyclops Integrator/C3) configured for measurement of  
125 chlorophyll *a*, colored dissolved organic matter (CDOM; measured via fluorescence proxy), and



126 turbidity was installed in the hull, behind the main keel, facing downwards. In all cases, fluorometric  
127 measurements are an imperfect measurement and are subject to artifacts. The chl. *a* and turbidity  
128 channels underwent single-point cross-calibration using a natural estuarine sample in the laboratory,  
129 referenced against a standard benchtop fluorometer that was recently calibrated. The CDOM channel  
130 was calibrated instead using the same estuarine water sample, but filtered. The response from the  
131 CDOM channel was calibrated using an associated absorption at 440 nm measured in a laboratory  
132 spectrophotometer with a 10 cm path length.

### 133 3 Assessment

#### 134 3.1 Vehicle performance

135 For the HAB monitoring trials, the *Nav2* vehicle was deployed from the beach three times between  
136 Dec. 18, 2017 and Feb. 7, 2018, for deployments of increasing length of one, three, and seven days  
137 (**Table 2; Figure 3**), in which case the boat traveled a total of 254 nautical miles (i.e. 470 km; 1 NM  
138 = 1.9 km) at an average rate of 1.0 knots (1 knot = 1 NM hr<sup>-1</sup>). Winds were relatively low during this  
139 time period, corresponding to an overall average of 6.3 knots as compared to average monthly Dec.  
140 and Jan. magnitudes of 10 to 13 knots<sup>1</sup>.

141 Each mission was operated in a similar manner. The initial waypoints were entered in advance via  
142 Wi-Fi using the chart-based app. Iridium satellite communication was used after deployment to  
143 monitor the vehicles progress and send updated waypoints as desired, but all navigation was  
144 controlled autonomously. To start each mission the *Nav2* was deployed from Sanibel Beach by hand  
145 rolling the ASV on its cart out to a depth of > 0.75 m, pointing it offshore, and providing a mild push.  
146 At the end of each mission the *Nav2* was directed to sail straight to shore until the keel grounded in  
147 shallow water. The *Nav2* was then placed back onto the wheel cart and pulled on-shore. For the 25-  
148 hour deployment beginning 2040 UTC Dec. 18, 2017 (**Figure 3a**), the *Nav2* was directed to head  
149 straight out and back; sailing first nearly due south to a point 10 NM offshore and then returning  
150 north to the beach. On the way back, in response to very calm winds, the thruster was turned on at  
151 minimal power to provide a speed of 1 knot which was enough to reach shore at a convenient time  
152 for pick up. Some drift was caused by local currents, which presents as a bend in the transect line.  
153 Despite the boat experiencing a near full tidal cycle in both the southward and northward direction of  
154 travel and experiencing winds between 0 and 3 knots for most of the deployment, the *Nav2* steadily  
155 progressed. This first short mission served as a data collection test of the fluorometer, which was  
156 logging to an SD card on board. For the 77-hour deployment beginning 1422 UTC Dec. 20, 2017  
157 (**Figure 3b**), the *Nav2* was again deployed directly from Sanibel Beach. The intent of this mission  
158 was to sail through an area with a known HABs bloom. The *Nav2* was directed to first travel south in  
159 a zig-zag pattern to cover increased area compared to the first deployment. In response to updated  
160 satellite imagery, the *Nav2* was then directed west 15 NM and then north returning to a convenient  
161 pick up location at the NE limits of Sanibel Island. The decision was made to persist with sail power  
162 for nearly the entire mission to better assess performance in the very calm wind conditions. Depending  
163 on solar gain and battery status the thruster can be used for up to 48+ continuous hours to complete  
164 straight transects in a timely manner. Tidal current drift effected the precision of transect lines when  
165 the wind was < 3 knots. The vessel was removed from the water mid-deployment by a recreational  
166 boater, who mistakenly assumed the vessel was lost, and who then traveled with the *Nav2* in a  
167 northwest direction for 5 km. The *Nav2* was tracked during this time and contact was established  
168 with the recreational boaters, who were instructed to place the vessel back into the water. At the end

---

<sup>1</sup> [https://www.windfinder.com/windstatistics/southwest\\_of\\_tampa\\_bay\\_buoy](https://www.windfinder.com/windstatistics/southwest_of_tampa_bay_buoy)

169 of this mission a more prominent statement was added to the Nav2's sail indicating boldly its nature  
170 as a tracked and monitored research vessel. No such problem has occurred since. Near the end of the  
171 mission the winds were calm and the thruster was used at low power to return in a timely manner for  
172 pickup at the beach. For the 148-hour deployment beginning 1841 UTC Jan. 31, 2018 (**Figure 3c**),  
173 the vessel was again deployed from Sanibel Beach with the intent of traversing a significant distance  
174 of the West Florida Shelf. The vessel traveled west around Sanibel Island and then proceeded  
175 northwards along the coast between 10 and 30 km offshore. After approaching Tampa Bay, the *Nav2*  
176 was given waypoints to perform several longitudinal transects, until eventually being directed to the  
177 south for retrieval at Venice Beach.

178 To evaluate the sailing capabilities of the *Nav2* vessel, a polar diagram was constructed (**Figure 4**).  
179 The diagram illustrates the obtained vessel speed as a function of realized apparent winds as sensed  
180 by the onboard wind sensor (**Figure 1**). For winds from angles directly behind the vessel to as far as  
181  $45^\circ$  into the wind while under waypoint navigation, the vessel autonomously steers directly to the  
182 desired destination and the colored lines represent Velocity Made good on Course (VMC). If the  
183 *Nav2* is traveling towards a desired waypoint that happens to be directly into the wind (with a  
184 threshold of  $45^\circ$  port or starboard), the vessel instead autonomously chooses to tack and achieves a  
185 net Velocity Made Good (VMG) towards the waypoint. Represented in Figure 4 are therefore two  
186 separate calculations; if winds are  $< 45^\circ$  off of the bow, the VMG instead represents the apparent  
187 velocity with respect to the destination. Increasing apparent wind velocities results in higher *Nav2*  
188 velocities for speeds at least as high as 25 knots, under which conditions the vessel is capable of  
189 traveling at average speeds  $> 2$  knots. The *Nav2* is capable of reaching average speeds  $> 1$  knot if  
190 winds are at least 5 to 10 knots and greater than  $60^\circ$  away from the wind. Under low wind conditions  
191  $< 5$  knots, the vessel realizes  $VMC/VMG > 0.5$  knots for all apparent wind directions  $> 30^\circ$ . Overall,  
192 the vessel is capable of realizing significant forward progress, regardless of wind direction, in all but  
193 the most unfavorable wind conditions ( $> 40 \text{ km day}^{-1}$ ).

194 To evaluate if there were effects of bubbles on the fluorometric data, the three measured parameters  
195 were binned according to the wind speed at the time of data collection (**Figure 5**). We are assuming  
196 in this case that higher wind speeds would generate more choppy ocean conditions and thus a larger  
197 number of bubbles which may provide measurement artifacts both attenuating and amplifying  
198 signals, depending on several factors. However, we observe that the fluorometric data does not  
199 appear to depend on wind speed. While there is an increase in chl *a*. values at lower apparent wind  
200 speeds, this is likely just coincident with the *Nav2* experiencing lower winds closer to shore in the  
201 first two deployments, in the presence of the confirmed algae bloom (described in the next section).

### 202 3.2 Harmful algal bloom monitoring

203 To determine if the *Nav2* is a viable platform for HAB detection and mapping, the chl. *a* data was  
204 used as a proxy to provide information regarding algal densities. The same 3-channel fluorometer  
205 was used as the primary detection means for chl. *a*. For the first two, shorter deployments, a large and  
206 intense *K. brevis* (Florida Red Tide) bloom was present near shore ( $\sim 2 \text{ km}$ ) towards which the vessel  
207 was directed (**Figure 6a&b**). These deployments were intended to demonstrate the potential of the  
208 *Nav2* for HAB mapping in localized areas in response to a bloom. The third deployment of 1-week  
209 duration on the other hand was intended to demonstrate the potential for the boat to be used for  
210 sustained, large-area HAB mapping, even in off-shore environments (**Figure 6c**). Generally, the  
211 spatial trends of the in situ fluorometric data agreed well with the results from satellite imagery;  
212 however, concentrations derived via remote sensing were significantly elevated compared to the in  
213 situ data. For all three deployments, elevated chl. *a* south/southwest of Sanibel Island was probably

214 due primarily to *K. brevis*, given that this species was identified locally at cell counts exceeding  
215 100,000 L<sup>-1</sup> (discrete samples in **Figure 6a-c**).

216 For the first deployment between Dec. 18 and 19, 2017 (**Figure 6a**), the vessel encountered an  
217 elevated chl. *a* patch ~2.5 km south of the beach deployment location. Peak in situ concentrations in  
218 the patch were ~ 6 µg L<sup>-1</sup> but were more typically between 1 and 3 µg L<sup>-1</sup>. Interestingly, the initial  
219 *Nav2* transect (i.e. southward) only recorded chl. *a* concentrations less than 1.5 µg L<sup>-1</sup>, illustrating the  
220 heterogeneity within the patch. In contrast, the remotely sensed background patch was larger and  
221 concentrations were higher, between 5 and 50 µg L<sup>-1</sup>. The second deployment between Dec. 20 and  
222 23, 2017 again revealed a high degree of spatial heterogeneity. For the first portion of the deployment  
223 chl. *a* concentrations rarely exceeded 2 µg L<sup>-1</sup>. After traveling further west, the vessel soon  
224 encountered two chl. *a* patches greater than 5 µg L<sup>-1</sup>. Satellite data did not display a high matchup in  
225 this case, as would be expected given that a 3-day composite was used; however, satellite data did  
226 reveal that elevated chl. *a* was also observed with a patchy distribution. For the final deployment  
227 beginning 5 weeks later between Jan. 31 and Feb. 6, 2018, in situ chl. *a* values were an order of  
228 magnitude lower than in Dec. 2017. Just south of Sanibel Island, chl. *a* approached as high as 0.4 µg  
229 L<sup>-1</sup>, but then remained less than 0.2 µg L<sup>-1</sup> for most of the remainder of the deployment. The higher  
230 values are consistent with the vessel being closer to shore, but also perhaps with a residual HAB  
231 bloom, albeit *K. brevis* cell counts were below detection to the west of the deployment location.  
232 While satellite chl. *a* was again much greater than the in situ *Nav2* data, its relative magnitude also  
233 decreased by approximately an order of magnitude, with concentrations ~5 µg L<sup>-1</sup> nearshore and less  
234 than 2 µg L<sup>-1</sup> for the offshore portion of the deployment. Interestingly, several portions of the color  
235 track show conspicuously less chl. *a* despite little variations in other parameters, e.g. depth. Upon  
236 further investigation, this phenomenon was revealed to be the result of diel variations (**Figure 7c**).  
237 Very distinct depressions of the chl. *a* signal were observed between the daylight hours of 1300 and  
238 2300 UTC (8:00 am and 6:00 pm locally). These variations are likely explainable by vertical diel  
239 migration (Haphey-Wood, 1976) or by variations in pigment expression or measurement artifacts  
240 (Babin et al., 1996). These intraday variations were not observed in other deployments where *K.*  
241 *brevis* was likely present (or in the very first day of the 2018 deployment near confirmed *K. brevis*),  
242 consistent with the knowledge that this organism does not migrate downwards during the day  
243 (Schofield et al., 2006).

244 Turbidity and chl *a*. data provide further information regarding the environmental context of these  
245 organisms (**Figure 8d-f**), as well as evidence for the proper functioning of the *Nav2*/fluorometer  
246 package, i.e. that the data is consistent with expectations. The CDOM data is represented as  
247 absorption at 440 nm despite being fluorometrically obtained. While this is not traditional, we argue  
248 that an estimation of CDOM absorption is arguably more useful than representing data in more  
249 traditional units (e.g. quinine-sulfate units), and a linear response would be expected either way.  
250 Thus, while the CDOM magnitude may not be completely accurate (although values between 0.05  
251 and 0.3 m<sup>-1</sup> are consistent with CDOM data measured at the Caloosahatchee River outflow)(Del  
252 Castillo et al., 2000b)), the spatial variance in the observed CDOM should in fact be accurate. For all  
253 three deployments, CDOM increased nearshore consistent with freshwater discharge from inlets,  
254 both at deployment and retrieval sites but also during mid-deployment transects (e.g. Feb. 2, 2018;  
255 **Figure 8f**). Other increases appear associated with *K. brevis* patches (based on the chl. *a* signature) or  
256 river plumes (e.g. Dec. 19, 2017; **Figure 8d**). Along these lines, in the absence of a bloom and in a  
257 coastline receiving discharge from a single freshwater source, the CDOM data may serve as a proxy  
258 for salinity. Turbidity, being measured as the amount of light scattered at 90° from a source at a  
259 single wavelength, appears to more reflect a combination of suspended sediment and phytoplankton



260 cells (**Figure 8g-i**). Turbidity measurements were more transient and less precise at a single location  
261 than CDOM (e.g. Feb 3,4, 2018; **Figure 8i**), consistent with transient suspended sediments and a  
262 heterogeneous water column. Winds were indeed in the 12 to 25 knot range Feb 3 from around UTC  
263 0600 to 2200, and then periodically elevated on Feb. 4 throughout the day, which could provide an  
264 explanation. Turbidity increases were also observed near *K. brevis* bloom patches (evidenced by  
265 elevated chl. *a*; **Figure 8g**). It is notable that CDOM measurements have a higher precision than the  
266 turbidity measurements (e.g. **Figure 8f&i**). This is expected because the dissolved CDOM will be  
267 much more homogeneously mixed than will particulates measured via turbidity.

## 268 4 Discussion

### 269 4.1 Platform functionality

270 Though three deployments of increasing duration, the *Nav2* autonomous sail vehicle successfully  
271 demonstrated the potential for the platform to provide mobile, unattended monitoring of the surface  
272 coastal ocean. The *Nav2* is a unique platform in that it is small enough to be deployed in coastal and  
273 inland waters, and by functioning identically to a real sailboat it can obtain high speeds and  
274 accurately navigate and map areas of interest. The deployments demonstrated the vessel is robust  
275 enough to reliably operate and survey under non-ideal sea states with winds up to 25 knots (although  
276 we have tested the vehicle in winds > 30 knots in coastal waters of New England and Washington  
277 State). Under conditions encountered in southwest Florida with winds averaging less than 4 knots,  
278 however, the boat still managed to cover 17 to 22 NM per day, and 29 NM per day with winds  
279 averaging 8 knots (**Table 2**). These winds were not necessarily directed from behind the boat; indeed,  
280 the vessel can sail into the wind via autonomous tacking, under which significant forward progress is  
281 still made at a VMG of 10 NM per day; **Figure 4**). The vessel is capable of efficiently reaching  
282 preselected (or adjusted on the fly) waypoints (**Figures 2&3**). On the other hand, during deployment  
283 and retrieval the boat can be operated manually in sailing mode, or with a thruster (**Table 2**). The  
284 thruster is particularly useful in areas of high currents or ship traffic. Using the thruster only, the  
285 *Nav2* can be used for short missions (up to 48 hours) without the sail.

286 We demonstrated deployments of up to one week. The vessel was operating exceptionally at the time  
287 of retrieval and could have continued longer. Indeed, *Nav2* deployments since the time of writing this  
288 report have lasted for 15+ days. Power efficiency improvements are ongoing with multi-sensor,  
289 multi-month mission lengths feasible. Approximately 1 to 5 Watts extra power is available for  
290 sensors. The power availability and length of mission will vary with solar conditions. In solar  
291 conditions typical of Florida the panels typically provide an average of 200 W hrs day<sup>-1</sup>. In low light  
292 conditions typical of northern latitudes in the winter, mission planning needs to be adjusted  
293 accordingly.

294 Deployment or retrieval of the *Nav2* is simple but exciting and can be achieved from a boat ramp or  
295 from the beach under calm seas by a single operator. All three deployments described herein were  
296 initiated from the beach. For deployment, the operator simply walks the small hand-held trailer into  
297 the surf zone into waist-deep water until it is floating, and then slides the trailer out from underneath  
298 the vessel. The operator can leave the iOS device on shore during the actual deployment or place it  
299 into a waterproof case and hold with a lanyard. For retrieval the vehicle can be lifted back onto its  
300 wheel cart by hand in shallow water and then pulled on shore. The *Nav2* is also capable of being  
301 lifted from the water directly from a small boat. An easily overlooked aspect of using the vehicle is  
302 the attention that it garners from beachgoers. This is an opportunity for community outreach, and the  
303 southwest Florida HAB monitoring deployments were met with great inquiry and enthusiasm,

304 eventually becoming the subject of several media features. Unfortunately, however, this curiosity  
305 also led to mission interruption on Dec. 22, 2017, when a recreational boater pulled the Nav2 from  
306 the water and proceeded towards shore until seeing the contact information and statement on the  
307 ASV. Under extremely low winds if the vessel is not obviously making forward progress it can  
308 appear “lost”. Of course, theft is always an issue, especially of a smaller 2 m length boat. Future  
309 versions of the vehicle are expected to be slightly larger to hold a larger number of sensors; this may  
310 also serve the dual purpose of being a theft deterrent. The “curiosity” effect has been better managed  
311 since these deployments by adding a large bold statement directly on the sail indicating the Nav2 is a  
312 “RESEARCH VESSEL” “TRACKED AND MONITORED AT ALL TIMES”. Boaters are  
313 increasingly aware that drones of all types on land or sea are carefully monitored. No problems with  
314 curiosity or theft have occurred since. Other ongoing improvements with the *Nav2* vehicle include an  
315 increased vehicle size to more easily accommodate a variety of sensors, the integration and testing of  
316 additional sensors, refinements to the autonomous steering algorithm to reduce oversteering and  
317 increase average speed, improved consistency of performing desirable straight data collection  
318 transects in variable currents., and improved power efficiency to provide greater power for sensors  
319 and in low light conditions.

## 320 4.2 Applications for Marine HAB monitoring.

321 The utility of the platform was demonstrated for the specific application of harmful algal bloom  
322 monitoring of the Florida Red Tide species *Karenia brevis*. The recurring *K. brevis* blooms ravaging  
323 southwest Florida are challenging to monitor because blooms are most detrimental nearshore, but in  
324 many cases are transported shoreward from deeper waters ((Vargo, 2009)). While depth-resolved  
325 measurements are ideal and have been routinely obtained by glider as part of the State of Florida  
326 monitoring program, gliders have difficulty operating in waters less than 10 m deep, especially in  
327 dynamic environments. Gliders are also more expensive to operate in shallow waters (they require  
328 more frequent attention and battery and buoyancy pump servicing), prohibiting continuous operation.  
329 Finally, gliders possess a limited selection of sensors and face many sensor design constraints,  
330 currently limiting the wide-use of species-level detection techniques. Regardless, by the time *K.*  
331 *brevis* blooms approach the coast, they are usually at the surface of a well-mixed water column and  
332 the need for depth-resolved measurements is decreased (Robbins et al., 2006). Thus, there will for the  
333 foreseeable future be a niche that must be filled for sustained coastal surface monitoring for this  
334 species.

335 While the work presented herein only used a chl. *a* sensor (a common glider sensor), results serve as  
336 justification for the investment into compatible HAB species-specific sensors. The fluorescence  
337 response of organic matter has been extensively used as a proxy since terrestrially-based coastal  
338 CDOM can, for discrete regions and time intervals, display nearly linear relationships with salinity  
339 and FDOM (Coble, 1996; Del Castillo et al., 2000a). The success of the platform/sensor combination  
340 is demonstrated by the matchup to satellite observations (**Figure 6**), repeatable diel variations  
341 (**Figure 7**), obtainment of reasonable ancillary fluorometric data (**Figure 8**), and a lack of discernible  
342 bubble artifacts (**Figure 5**). Interestingly, the chl. *a* data obtained in situ was of much lower  
343 concentration than that detected by satellite. These variations can be expected based on the different  
344 nature of the measurements. The fluorometric measurements of chl. *a* can be subject to various  
345 packaging effects, especially at higher concentrations, and numerous accessory pigments can also  
346 contribute to the signal (Babin et al., 1996; Schofield et al., 2006). Satellite measurements, on the  
347 other hand, integrate over a depth interval and calculated concentrations are therefore representative  
348 of an average concentration of the surface water column. They are also more challenging in turbid  
349 and CDOM-rich optically complex waters where we conducted the deployments (Hu et al., 2005).

350 With a fleet of *Nav2* vehicles traveling ~20 NM per day in a repeatable triangular or “lawnmower”  
351 raster pattern, several vehicles have the potential to continuously survey a large area, regardless of  
352 water depth. The *Nav2* can also reveal more *K. brevis* surface heterogeneity than remote sensing data,  
353 and data is acquired at a much greater temporal resolution. Therefore, the *Nav2*/fluorometer package  
354 has the potential to provide satellite remote sensing ground-truthing data that can be used to improve  
355 the species-specific algorithms. An unexpected result were the repeatable diel variations observed  
356 during the longer mission (**Figure 7c**). Similar results have been observed in the same region of the  
357 surface ocean during glider missions (unpublished). While not consistent with the behavior of *K.*  
358 *brevis* cells, which instead exhibit positive phototaxis during the daylight hours (Schofield et al.,  
359 2006), the resident phytoplankton appear to be either altering their surface expression of chl. *a* in an  
360 excess of light or are descending to deeper waters, e.g. to obtain nutrients or alleviate photo stress  
361 (Vargo, 2009). Overall, the high sensitivity and reproducibility of the measurements highlight the  
362 functionality of the sensor for high precision measurements.

### 363 4.3 Other monitoring applications.

364 While chl. *a* measurements were the primary focus of this project, the ancillary fluorometric data  
365 streams also shed light on some in water processes and allude to future applications of the *Nav2*  
366 vessel. CDOM is of interest to biogeochemists for its role in dominating ocean color, playing a  
367 critical role in photobiology, photochemistry (Helms et al., 2008), and photoproduction of CO<sub>2</sub>  
368 (Clark et al., 2004), contributing to aspects of the oceanic sulfur cycle (Gali et al., 2016), and  
369 controlling the absorption of light energy and the subsequent impacts on heat flux (Hill, 2008) and  
370 other ocean-climate interactions, and in serving as a tracer of freshwater (Fichot and Benner, 2012).  
371 The fluorometrically measured CDOM exhibited intensities and spatial concentration distributions  
372 that are expected in southwest Florida (Del Castillo et al., 2000a). Earlier in the project, we did install  
373 a conductivity-temperature-depth CTD package onto the vehicle. However, conductivity  
374 measurements were unreasonable, likely due to bubble retention in the flow cell. While we still aim  
375 to resolve this issue with a different installation configuration, we can instead use CDOM as a rough  
376 proxy for salinity, with the assumption that there is a single source of freshwater input that has a high  
377 CDOM concentration (i.e. the Charlotte Harbor and the Caloosahatchee River).

378 The *Nav2* is inherently a meteorological sensor (e.g. for wind speed and magnitude, atmospheric  
379 temperature, and humidity). Previously, the *Nav2* has been successfully configured with fisheries  
380 sensors, including a pinger tracking hydrophone system (Sonotronics) and a cetacean and noise  
381 monitoring hydrophone (Song Meter). Trials demonstrated successful location of crab tracking  
382 pingers on the Washington coast and acoustic detection of various cetacean species. As of the time of  
383 writing, we are currently adding a Wetlabs BB3 Scatterometer and a Solinst CT logger for HABs  
384 surveys on Lake Okeechobee and the Indian River Lagoon in Florida. Addition of Oxygen/Temp  
385 Optode (Aanderaa AADI) and CT sensors as well as an ADCP (Nortec) are under consideration to  
386 provide a complete water quality monitoring suite.

## 387 5 Conclusions

388 The Navocean autonomous sail vehicle (*Nav2*) has been demonstrated to serve as a reliable mobile  
389 platform for wide-area surface coastal monitoring. To our knowledge, this is the first demonstration  
390 of a sail-driven vessel used for coastal HAB monitoring. The scientific results were shown to be  
391 reasonable and have the potential to map HAB blooms and associated environmental conditions.  
392 While the *Nav2* does not capture depth variations or collect instantaneous large surface area  
393 measurements as do underwater gliders and satellites, respectively, the platform is a useful tool in the

394 arsenal for coastal or inland monitoring. The primary benefits of using the *Nav2* vehicle are that it is  
395 fast and has reliable, autonomous navigation, has a completely renewable power source with no  
396 consumables, can function in shallow or deep water inland or offshore, and is operable by a single  
397 person. There are several additional demonstrated payload options as well as some currently in  
398 preparation. At least with the planar-style optical sensors, bubbles do not appear to contribute  
399 significant artifacts.

400 Harmful cyanobacterial blooms are increasing in intensity in global freshwater bodies (Paerl et al.,  
401 2018). The *Nav2* vehicle is ideal for monitoring blooms in these frequently shallow lakes, especially  
402 by limnologists who may have less training with more traditional oceanographic tools. To this end,  
403 we are readying for deployments for freshwater *Microcystis aeruginosa* HAB monitoring in Lake  
404 Okeechobee in the winter 2018-2019. Until the summer of 2018, there were few traditional  
405 monitoring efforts, and no real-time water quality monitoring sensors on Lake Okeechobee, and even  
406 now, only one stationary optical sensor is providing ground-truthing data for satellite efforts. We plan  
407 to augment this fixed location monitoring with *Nav2* surveys to both add a mobile monitoring  
408 element, but also to constrain the spatial variability of the surface optical properties in relation to  
409 remote sensing data. A second 3-channel fluorometer is currently being installed to provide  
410 phycoyanin and phycoerythrin measurements that help discriminate multiple algal species.  
411 Eventually, we envision the *Nav2* platform as an essential part of multiple monitoring programs.

## 412 **6 Acknowledgements**

413 We would like to thank L. Kellie Dixon, Jim Hillier, and Karl Henderson at Mote, and last but not  
414 least our former high school intern Gabriel Rey for assistance with field work.

## 415 **7 Conflict of Interest**

416 *The authors declare that the research was conducted in the absence of any commercial or financial*  
417 *relationships that could be construed as a potential conflict of interest.*

## 418 **8 Author Contributions**

419 JB authored the manuscript, provided scientific oversight, and participated in field campaigns, EA is  
420 the lead designer of the autonomous vehicle hardware and software, RC developed live data  
421 visualization interface, EM coordinated field campaigns, and SD designed the sailboat and conducted  
422 deployments.

## 423 **9 Funding**

424 This work was supported in part by a National Academies Gulf Research Program Early Career  
425 Fellowship award #2000007281 that supporting salary and supplies, and the Gulf of Mexico Coastal  
426 Ocean Observation System #NA16NOS0120018 that supported salaries.

## 427 **10 Data Availability Statement**

428 All datasets generated for this study are included in the manuscript and the supplementary files.



429 **11 References**

- 430 Anderson, D.M., Glibert, P.M. and Burkholder, J.M. (2002) Harmful algal blooms and  
431 eutrophication: Nutrient sources, composition, and consequences. *Estuaries* 25, 704-726.
- 432 Babin, M., Morel, A. and Gentili, B. (1996) Remote sensing of sea surface Sun-induced chlorophyll  
433 fluorescence: consequences of natural variations in the optical characteristics of phytoplankton and  
434 the quantum yield of chlorophyll a fluorescence. *International Journal of Remote Sensing* 17, 2417-  
435 2448.
- 436 Backer, L.C., McNeel, S.V., Barber, T., Kirkpatrick, B., Williams, C., Irvin, M., Zhou, Y., Johnson,  
437 T.B., Nierenberg, K., Aibel, M., LePrell, R., Chapman, A., Foss, A., Corum, S., Hill, V.R., Kieszak,  
438 S.M. and Cheng, Y.-S. (2010) Recreational exposure to microcystins during algal blooms in two  
439 California lakes. *Toxicon* 55, 909-921.
- 440 Bowers, H. and Smith, G.J. (2017) Sensors for Monitoring of Harmful Algae, Cyanobacteria and  
441 Their Toxins, in: Technologies, A.f.C. (Ed.), Workshop Proceedings. Moss Landing Marine  
442 Laboratories, Moss Landing, CA.
- 443 Brand, L.E. and Compton, A. (2007) Long-term increase in *Karenia brevis* abundance along the  
444 Southwest Florida Coast. *Harmful Algae* 6, 232-252.
- 445 Carmichael, W.W. (2001) Health Effects of Toxin-Producing Cyanobacteria: “The CyanoHABs”.  
446 *Human and Ecological Risk Assessment: An International Journal* 7, 1393-1407.
- 447 Clark, C.D., Hiscock, W.T., Millero, F.J., Hitchcock, G., Brand, L., Miller, W.L., Ziolkowski, L.,  
448 Chen, R.F. and Zika, R.G. (2004) CDOM distribution and CO<sub>2</sub> production on the southwest Florida  
449 shelf. *Marine Chemistry* 89, 145-167.
- 450 Coble, P.G. (1996) Characterization of marine and terrestrial DOM in seawater using excitation  
451 emission matrix spectroscopy. *Marine Chemistry* 51, 325-346.
- 452 Daniel, T., Manley, J. and Trenaman, N. (2011) The Wave Glider: enabling a new approach to  
453 persistent ocean observation and research. *Ocean Dynamics* 61, 1509-1520.
- 454 Del Castillo, C.E., Gilbes, F., Coble, P.G. and Muller-Karger, F.E. (2000a) On the dispersal of  
455 riverine colored dissolved organic matter over the West Florida Shelf. *Limnology and Oceanography*  
456 45, 1425-1432.
- 457 Del Castillo, C.E., Gilbes, F., Coble, P.G. and Müller-Karger, F.E. (2000b) On the dispersal of  
458 riverine colored dissolved organic matter over the West Florida Shelf. *Limnology and Oceanography*  
459 45, 1425-1432.
- 460 Ducharme, J. (2018) Red Tide Is Killing Marine Life and Scaring Away Tourists in Florida. Here's  
461 What to Know About It, *Time Magazine Online*.
- 462 Fichot, C.G. and Benner, R. (2012) The spectral slope coefficient of chromophoric dissolved organic  
463 matter (S<sub>275–295</sub>) as a tracer of terrigenous dissolved organic carbon in river-influenced ocean  
464 margins. *Limnology and Oceanography* 57, 1453-1466.



- 465 Fleming, L.E., Rivero, C., Burns, J., Williams, C., Bean, J.A., Shea, K.A. and Stinn, J. (2002) Blue  
466 green algal (cyanobacterial) toxins, surface drinking water, and liver cancer in Florida. *Harmful*  
467 *Algae* 1, 157-168.
- 468 Gali, M., Kieber, D.J., Romera-Castillo, C., Kinsey, J.D., Devred, E., Perez, G.L., Westby, G.R.,  
469 Marrase, C., Babin, M., Levasseur, M., Duarte, C.M., Agusti, S. and Simo, R. (2016) CDOM Sources  
470 and Photobleaching Control Quantum Yields for Oceanic DMS Photolysis. *Environmental Science &*  
471 *Technology* 50, 13361-13370.
- 472 Gannon, D.P., Berens McCabe, E.J., Camilleri, S.A., Gannon, J.G., Brueggen, M.K., Barleycorn,  
473 A.A., Palubok, V.I., Kirkpatrick, G.J. and Wells, R.S. (2009) Effects of *Karenia brevis* harmful algal  
474 blooms on nearshore fish communities in southwest Florida. *Marine Ecology Progress Series* 378,  
475 171-186.
- 476 Happey-Wood, C.M. (1976) Vertical migration patterns in phytoplankton of mixed species  
477 composition. *British Phycological Journal* 11, 355-369.
- 478 Helms, J.R., Stubbins, A., Ritchie, J.D., Minor, E.C., Kieber, D.J. and Mopper, K. (2008) Absorption  
479 spectral slopes and slope ratios as indicators of molecular weight, source, and photobleaching of  
480 chromophoric dissolved organic matter. *Limnology and Oceanography* 53, 955-969.
- 481 Hill, V.J. (2008) Impacts of chromophoric dissolved organic material on surface ocean heating in the  
482 Chukchi Sea. *Journal of Geophysical Research-Oceans* 113, 10.
- 483 Hoagland, P., Jin, D., Polansky, L.Y., Kirkpatrick, B., Kirkpatrick, G., Fleming, L.E., Reich, A.,  
484 Watkins, S.M., Ullmann, S.G. and Backer, L.C. (2009) The Costs of Respiratory Illnesses Arising  
485 from Florida Gulf Coast *Karenia brevis* Blooms. *Environmental Health Perspectives* 117, 1239-1243.
- 486 Hu, C., Muller-Karger, F.E., Taylor, C., Carder, K.L., Kelble, C., Johns, E. and Heil, C.A. (2005)  
487 Red tide detection and tracing using MODIS fluorescence data: A regional example in SW Florida  
488 coastal waters. *Remote Sensing of Environment* 97, 311-321.
- 489 Kirkpatrick, B., Fleming, L.E., Backer, L.C., Bean, J.A., Tamer, R., Kirkpatrick, G., Kane, T.,  
490 Wanner, A., Dalpra, D., Reich, A. and Baden, D.G. (2006) Environmental exposures to Florida red  
491 tides: Effects on emergency room respiratory diagnoses admissions. *Harmful Algae* 5, 526-533.
- 492 McCabe, R.M., Hickey, B.M., Kudela, R.M., Lefebvre, K.A., Adams, N.G., Bill, B.D., Gulland,  
493 F.M.D., Thomson, R.E., Cochlan, W.P. and Trainer, V.L. (2016) An unprecedented coastwide toxic  
494 algal bloom linked to anomalous ocean conditions. *Geophysical Research Letters* 43, 10,366-  
495 310,376.
- 496 Mordy, C.W., Cokelet, E.D., De Robertis, A., Jenkins, R., Kuhn, C.E., Lawrence-Slavas, N.,  
497 Berchok, C.L., Crance, J.L., Sterling, J.T., Cross, J.N., Stabeno, P.J., Meinig, C., Tabisola, H.M.,  
498 Burgess, W. and Wangen, I. (2017) *Advances in Ecosystem Research*
- 499 *Saildrone Surveys of Oceanography, Fish, and Marine Mammals in the Bering Sea. Oceanography*  
500 30, 113-115.
- 501 O'Neil, J.M., Davis, T.W., Burford, M.A. and Gobler, C.J. (2012) The rise of harmful cyanobacteria  
502 blooms: The potential roles of eutrophication and climate change. *Harmful Algae* 14, 313-334.

## Autonomous Sail-Powered Surface Vehicle Harmful Algal Bloom Monitoring

- 503 Paerl, H.W., Otten, T.G. and Kudela, R. (2018) Mitigating the Expansion of Harmful Algal Blooms  
504 Across the Freshwater-to-Marine Continuum. *Environmental Science & Technology* 52, 5519-5529.
- 505 Reich, A., Lazensky, R., Faris, J., Fleming, L.E., Kirkpatrick, B., Watkins, S., Ullmann, S., Kohler,  
506 K. and Hoagland, P. (2015) Assessing the impact of shellfish harvesting area closures on neurotoxic  
507 shellfish poisoning (NSP) incidence during red tide (*Karenia brevis*) blooms. *Harmful Algae* 43, 13-  
508 19.
- 509 Robbins, I.C., Kirkpatrick, G.J., Blackwell, S.M., Hillier, J., Knight, C.A. and Moline, M.A. (2006)  
510 Improved monitoring of HABs using autonomous underwater vehicles (AUV). *Harmful Algae* 5,  
511 749-761.
- 512 Schofield, O., Kerfoot, J., Mahoney, K., Moline, M., Oliver, M., Lohrenz, S. and Kirkpatrick, G.  
513 (2006) Vertical migration of the toxic dinoflagellate *Karenia brevis* and the impact on ocean optical  
514 properties. *Journal of Geophysical Research: Oceans* 111.
- 515 Scholin, C.A., Gulland, F., Doucette, G.J., Benson, S., Busman, M., Chavez, F.P., Cordaro, J.,  
516 DeLong, R., De Vogelaere, A., Harvey, J., Haulena, M., Lefebvre, K., Lipscomb, T., Loscutoff, S.,  
517 Lowenstine, L.J., Marin Iii, R., Miller, P.E., McLellan, W.A., Moeller, P.D.R., Powell, C.L., Rowles,  
518 T., Silvagni, P., Silver, M., Spraker, T., Trainer, V. and Van Dolah, F.M. (2000) Mortality of sea  
519 lions along the central California coast linked to a toxic diatom bloom. *Nature* 403, 80.
- 520 Shapiro, J., Dixon, L.K., Schofield, O.M., Kirkpatrick, B. and Kirkpatrick, G.J. (2015) Chapter 18 -  
521 New Sensors for Ocean Observing: The Optical Phytoplankton Discriminator, in: Liu, Y., Kerkering,  
522 H., Weisberg, R.H. (Eds.), *Coastal Ocean Observing Systems*. Academic Press, Boston, pp. 326-350.
- 523 Smith, D.R., King, K.W. and Williams, M.R. (2015) What is causing the harmful algal blooms in  
524 Lake Erie? *Journal of Soil and Water Conservation* 70, 27A-29A.
- 525 Stockley, N.D., Sullivan, J.M., Hanisak, D. and McFarland, M.N. (2018) Using observation networks  
526 to examine the impact of Lake Okeechobee discharges on the St. Lucie Estuary, Florida, SPIE  
527 Defense + Security. SPIE, p. 8.
- 528 Vargo, G.A. (2009) A brief summary of the physiology and ecology of *Karenia brevis* Davis (G.  
529 Hansen and Moestrup comb. nov.) red tides on the West Florida Shelf and of hypotheses posed for  
530 their initiation, growth, maintenance, and termination. *Harmful Algae* 8, 573-584.
- 531

532 Table 1 – Specifications for the *Nav2* Autonomous Sail Vehicle (Navocean).

<b>Nav2 ASV Specifications and Capabilities</b>	
Mission Duration	Up to 6 months
Speed	1-3 Knots
Length	2m (6.5')
Draft	.75m (2.5')
Weight	85 lbs plus payload
Rigging	Main + Jib "storm" sails and chafe resistant lines
Mast	Unstayed reinforced carbon
Winch	Electric with anti-jamming spool
Rudder and Keel	No-tangle design sheds lines and seaweed
Power	12 Volt, 35 W solar array
Batteries	Up to 120 Ah LiFePO4
Standard Sensors	GPS, PRH, Meteorological, AIS
Optional Sensors	Water Quality: O <sub>2</sub> , CT, backscatter, 3/6 channel fluorometer (chl. a, phycocyanin, phycoerythrin, CDOM, turbidity, oil) Acoustic: Pinger Tracking, Cetaceans, Telemetry Custom: ADCP and many others
Navigation	Autonomous to waypoints + manual option
Charts	NOAA RNC included
UI	Chart based iOS App + web portal
Dashboard	Location, speed, course, heading, true and apparent wind, pitch, roll, power, battery and solar voltage, sail and rudder position, thruster RPM, connectivity status, waypoint ETA
Comms	Iridium SBD (Sat), Cell, and WiFi
Real-time	Configurable telemetry and sensor data

533

534

535

536

## Autonomous Sail-Powered Surface Vehicle Harmful Algal Bloom Monitoring

537 Table 2 – Summary of the environmental conditions and the *Nav2* ASV performance during harmful  
538 algae bloom tracking deployments. The distance covered includes periods of using the thruster at low  
539 speeds (~ 1 knot) in calm winds to return the ASV to shore for a convenient pickup time.  
540 Alternatively, the thruster can be used temporarily to complete important transects if the wind dies or  
541 for entire short missions of ~ 1 day.

MISSION DATES	NUMBER OF HOURS	WIND SPEED AVERAGE (Apparent)	BOAT SPEED AVERAGE (Knots)	SEA STATE BEAUFORT (Range)	DISTANCE COVERED (NM)	Percent Thruster Use
Dec 18 to 19, 2017	25	3.2	0.9	0-2	22.5	12%
Dec 21 to 24, 2017	77	3.6	0.7	0-3	53.9	10%
Jan 31 to Feb 06, 2018	148	8.2	1.2	0-5	177.6	3%

542

In review

543 **Figure Captions**

544 Figure 1 – Diagram of the Navocean Nav2 Autonomous Sail Vehicle and components.

545 Figure 2 – Screenshots of the iOS control software running on an iPad, illustrating operation via  
546 Manual Control (A) or via Waypoint navigation (B).

547 Figure 3 – Screenshots of the iOS control software running on an iPad, illustrating the three ASV  
548 tracks in southwest Florida for the purposes of harmful algal bloom monitoring from deployments  
549 between (A) Dec. 18 and 19, 2017, (B) Dec. 20 and 23, 2017, and (C) Jan. 31 and Feb. 6, 2018.  
550 Waypoints

551 Figure 4 – A polar diagram illustrating averaged *Nav2* velocity magnitude while sailing as a function  
552 of apparent wind magnitude and direction for all deployments. The four colors represent data for  
553 intervals for binned wind speeds. Between angles of 45° and 180°, the magnitude is the actual  
554 realized velocity over ground of the vehicle in the intended direction, or the “Velocity Made Good on  
555 Course”. The *Nav2* tacks as does a traditional sailboat at wind angles < 45°, realizing VMG  
556 (“Velocity Made Good”), and the vessel makes significant forward progress even when traveling at  
557 very low angles relative to the wind.

558 Figure 5 – For all deployments, the fluorometer data were binned by their associated 5-knot interval  
559 apparent winds speeds to determine if wind and associated bubbles exhibited an artifact.

560 Figure 6 – *Chl. a* colormaps or colortracks are presented as demonstrating of HAB mapping  
561 capabilities from the three *Nav2* deployments. Background MODIS satellite image is courtesy of Dr.  
562 Chuanmin Hu at University of South Florida, and the *K. brevis* cell count data was collected as part  
563 of the Florida Fish and Wildlife Commission / Mote Marine Red Tide Monitoring Partnership. The  
564 single return raster leg from the deployment during Dec. 18 to 19, 2017 warrants data representation  
565 as an interpolated colormap (between 0 and 4  $\mu\text{g L}^{-1}$ ) with an overlain boat track (black line), (A); A  
566 colortrack is used to represent (B) the Dec. 20-23, 2017 data (between 0 and 4  $\mu\text{g L}^{-1}$ ), and (C) the  
567 Jan. 31 – Feb. 6, 2018 data (between 0 and 0.4  $\mu\text{g L}^{-1}$ ). The background MODIS images are 1-, 3-,  
568 and 7-day composites, respectively, and the colors in all represent between 0 and 60  $\mu\text{g L}^{-1}$  remotely-  
569 sensed *chl. a* (Note: gray colors indicate areas with cloud cover and no data). Discrete samples  
570 collected and enumerated for *K. brevis* cells within 1 week of the deployments are represented by  
571 circular icons: grey indicates not present/background levels, white indicates very low densities  
572 >1,000-10,000 cells  $\text{L}^{-1}$ , yellow indicates low densities 10,000 – 100,000 cells  $\text{L}^{-1}$ , orange indicates  
573 medium densities 100,000 – 1,000,000 cells  $\text{L}^{-1}$ , and red indicates high > 1,000,000 cells  $\text{L}^{-1}$ .

574 Figure 7 –To examine diel trends, daily time series for *chl. a* are presented for the (A) Dec. 18-19,  
575 2017, (B) Dec. 20-23, 2017, and (C) Jan. 31 – Feb. 6, 2018 deployments. Multiple days are depicted  
576 on the same plots. Note, the y-axis magnitudes are different for the Jan. 31 to Feb. 6, 2018  
577 deployment.

578 Figure 8 – For the Dec. 18 to 19, 2017, Dec. 20 to 23, 2017, and Jan. 31 to Feb. 6, 2018 deployments,  
579 the *chl. a* time series is represented in (A) – (C) respectively, CDOM measured via fluorometric  
580 proxy is represented in (D) – (F) (explanation in text), and turbidity is represented in (G) – (I). Note,  
581 the y-axis magnitudes are different for the Jan. 31 to Feb. 6, 2018 deployment.



Figure 1.JPEG

bioRxiv preprint doi: <https://doi.org/10.1101/473827>; this version posted November 19, 2018. The copyright holder for this preprint (which was not certified by peer review) is the author/funder, who has granted bioRxiv a license to display the preprint in perpetuity. It is made available under aCC-BY-NC-ND 4.0 International license.

Figure 1

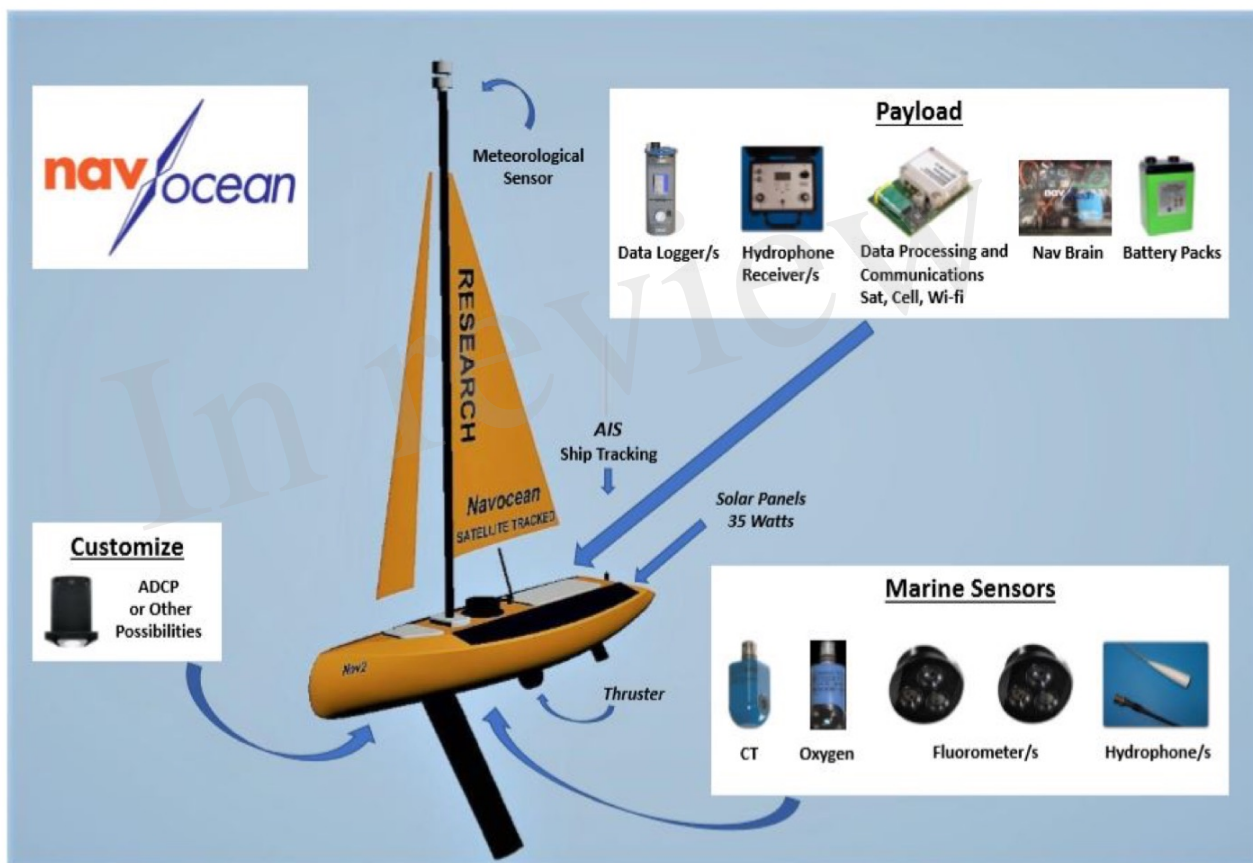


Figure 2.JPEG

bioRxiv preprint doi: <https://doi.org/10.1101/473827>; this version posted November 19, 2018. The copyright holder for this preprint (which was not certified by peer review) is the author/funder, who has granted bioRxiv a license to display the preprint in perpetuity. It is made available under aCC-BY-NC-ND 4.0 International license.

Figure 2

a)



b)

The 'NEW ACTION' screen includes the following fields and options:

- Waypoint:** Lat [ ] °, Lon [ ] °, rad 400 m, (optional name) ABCDEF, tack cor 30... m
- Set Course:** [ ] °
- Point Upwind:**
- Full Stop:**
- Start Over at #:** 1, repeat 7 times
- Buttons:** SAVE, Cancel

Figure 3.JPEG

bioRxiv preprint doi: <https://doi.org/10.1101/473827>; this version posted November 19, 2018. The copyright holder for this preprint (which was not certified by peer review) is the author/funder, who has granted bioRxiv a license to display the preprint in perpetuity. It is made available under aCC-BY-NC-ND 4.0 International license.

Figure 3

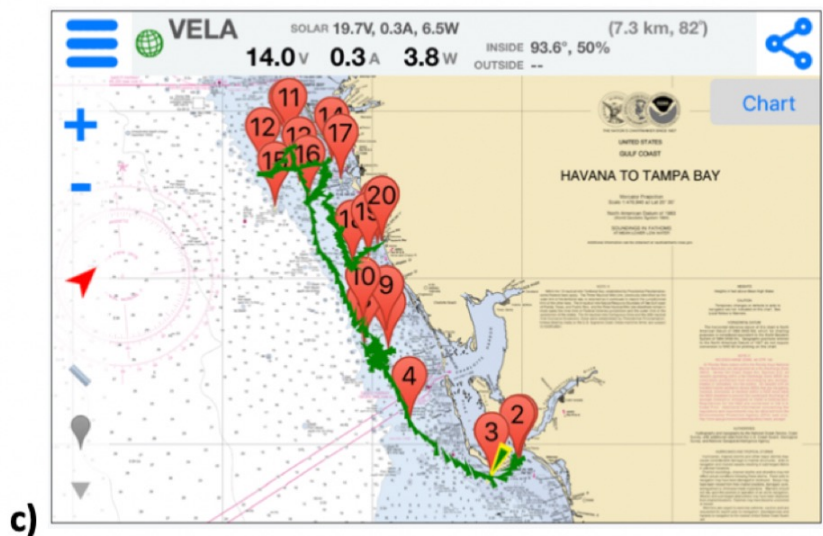
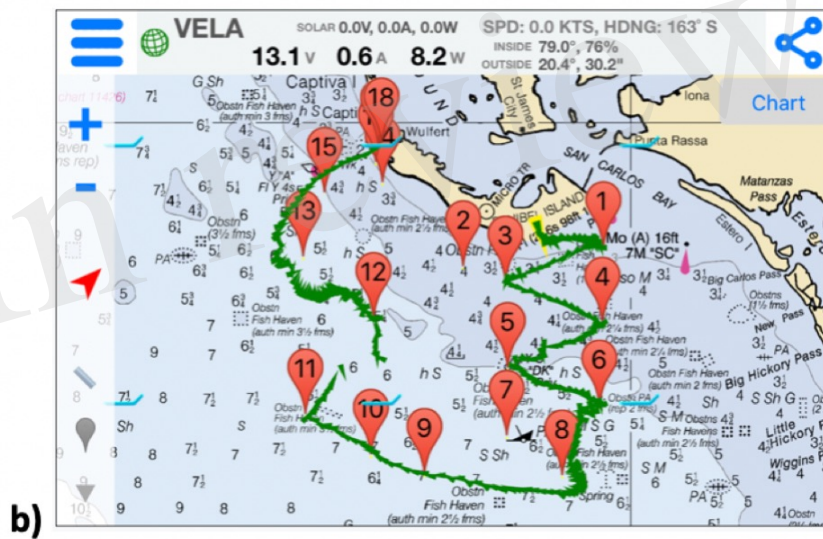
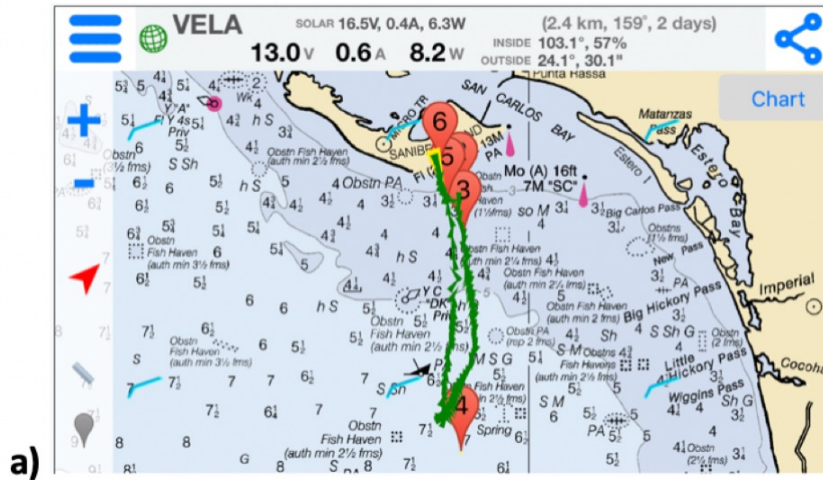


Figure 4.JPEG

bioRxiv preprint doi: <https://doi.org/10.1101/473827>; this version posted November 19, 2018. The copyright holder for this preprint (which was not certified by peer review) is the author/funder, who has granted bioRxiv a license to display the preprint in perpetuity. It is made available under aCC-BY-NC-ND 4.0 International license.

Figure 4

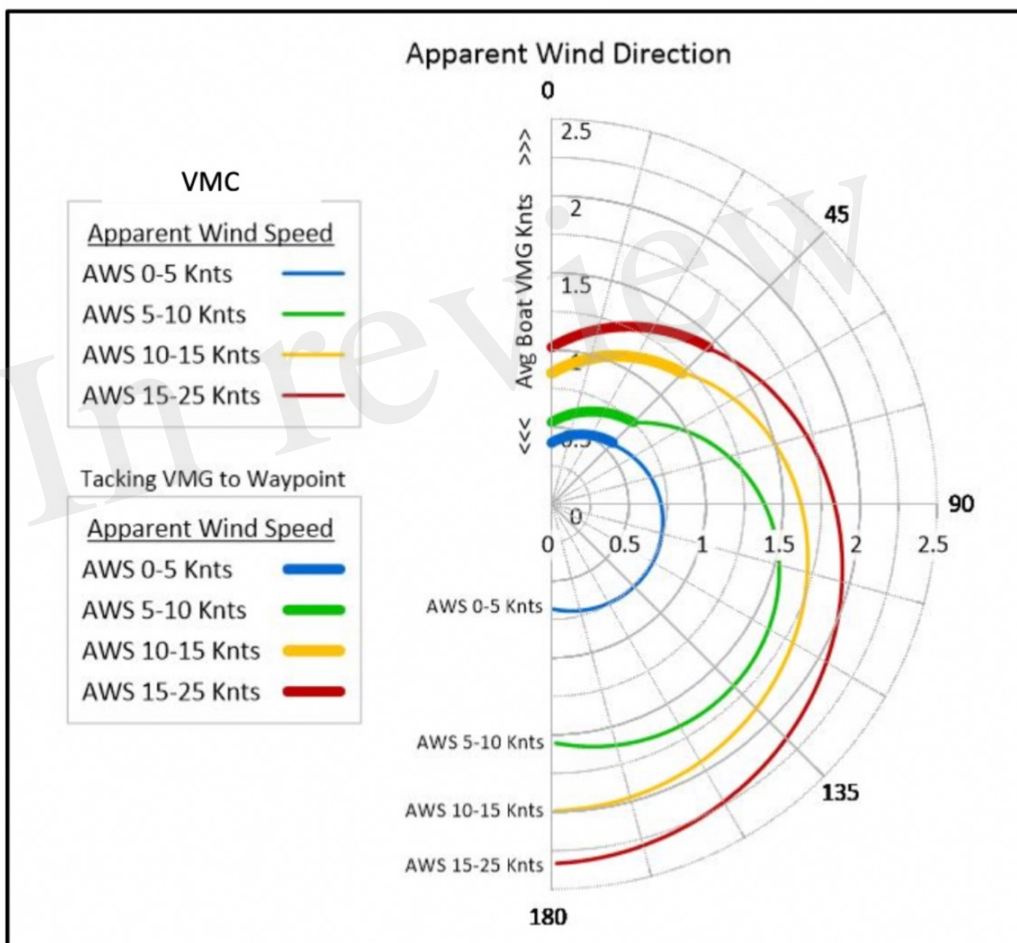


Figure 5.JPEG

bioRxiv preprint doi: <https://doi.org/10.1101/473827>; this version posted November 19, 2018. The copyright holder for this preprint (which was not certified by peer review) is the author/funder, who has granted bioRxiv a license to display the preprint in perpetuity. It is made available under aCC-BY-NC-ND 4.0 International license.

Figure 5

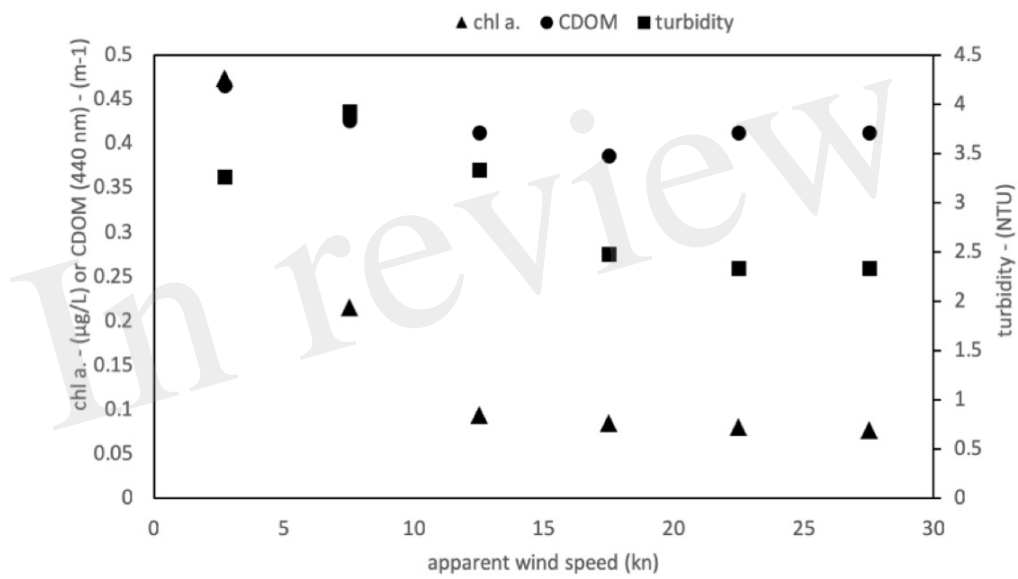
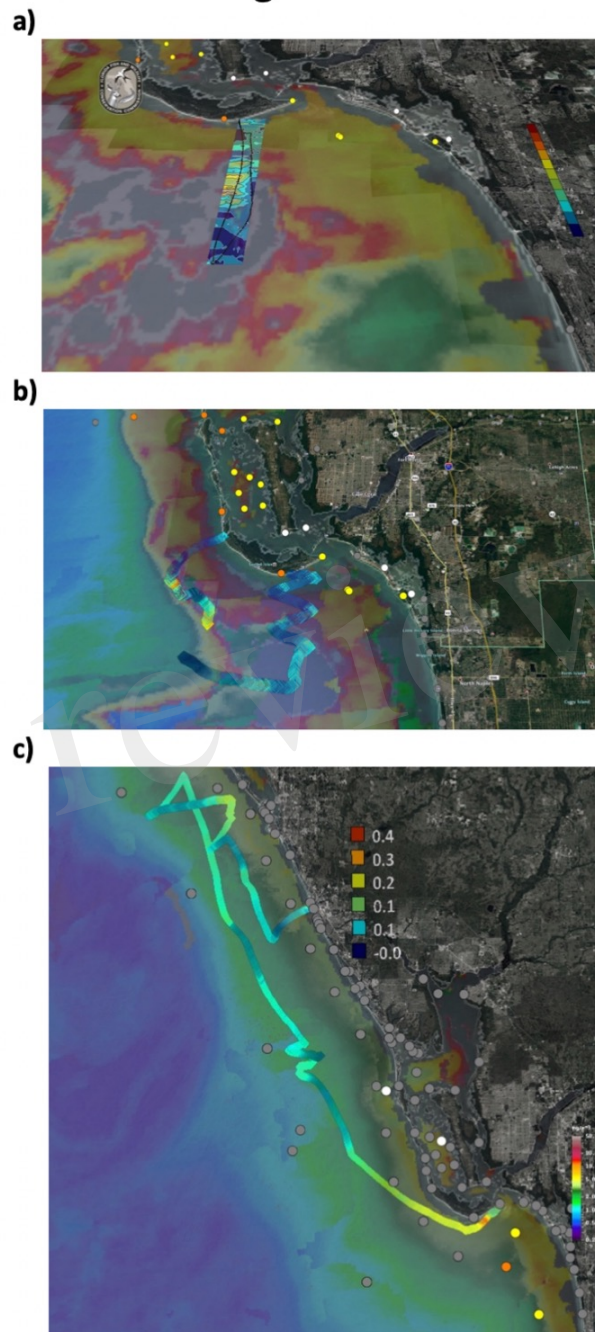




Figure 6.JPEG

bioRxiv preprint doi: <https://doi.org/10.1101/473827>; this version posted November 19, 2018. The copyright holder for this preprint (which was not certified by peer review) is the author/funder, who has granted bioRxiv a license to display the preprint in perpetuity. It is made available under aCC-BY-NC-ND 4.0 International license.

Figure 6



bioRxiv preprint doi: <https://doi.org/10.1101/473827>; this version posted November 19, 2018. The copyright holder for this preprint (which was not certified by peer review) is the author/funder, who has granted bioRxiv a license to display the preprint in perpetuity. It is made available under aCC-BY-NC-ND 4.0 International license.

Figure 7

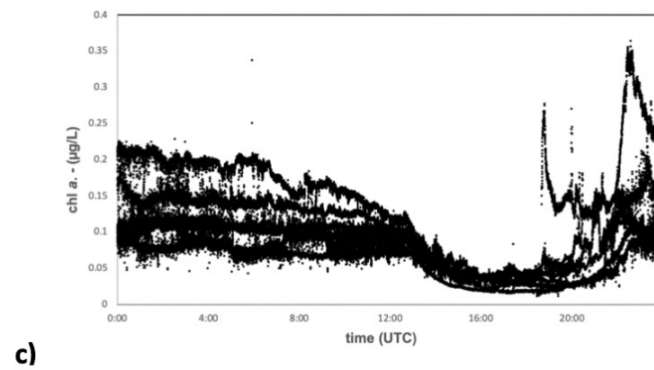
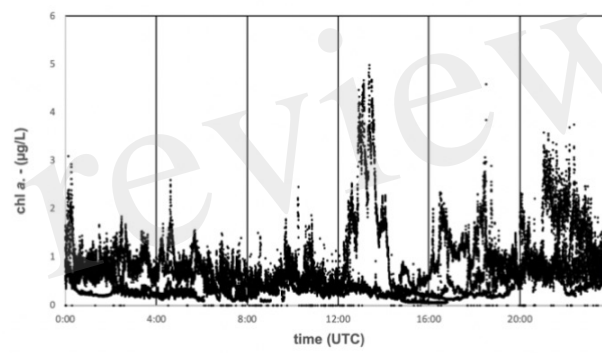
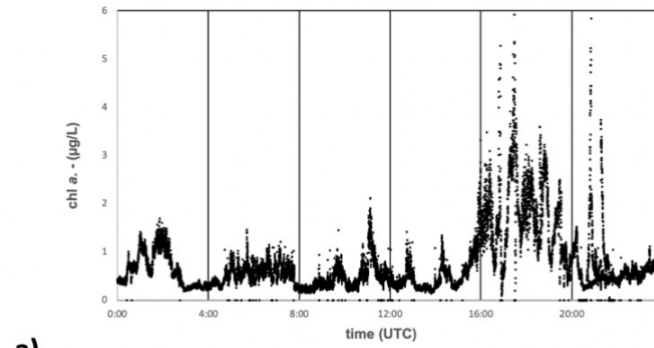


Figure 8.JPEG

bioRxiv preprint doi: <https://doi.org/10.1101/473827>; this version posted November 19, 2018. The copyright holder for this preprint (which was not certified by peer review) is the author/funder, who has granted bioRxiv a license to display the preprint in perpetuity. It is made available under aCC-BY-NC-ND 4.0 International license.

Figure 8

